Obtaining and characterization of Ni-Zr type amorphous tapes

L. BÜKKÖSI*, GY. THALMAIER, C. CODREAN[a], P. PĂȘCUȚĂ[b], I. VIDA-SIMITI
Department of Materials Science and Technology, Technical University of Cluj-Napoca, 103-105 Muncii Ave., 400641 Cluj-Napoca, Romania
[a]*Mechanical Faculty, Politehnica University of Timisoara, 1 Mihai Viteazu Ave., 300222 Timisoara, Romania*
[b]*Department of Physics and Chemistry, Technical University of Cluj-Napoca, 103-105 Muncii Ave., 400641 Cluj – Napoca, Romania*

The NiZr master alloys were prepared by arc melting using high purity metals in a Ti-gettered argon atmosphere. The alloys were melted several times in order to improve homogeneity. The ingots were induction-melted under a high-purity argon atmosphere in a quartz tube and a graphite crucible, injected through a nozzle onto a Cu wheel to produce rapidly solidified amorphous ribbons. The characterization of the amorphous ribbons was done by X-ray diffraction, DSC analysis and tensile tests. The crystallization of amorphous $Ni_{64}Zr_{36}$ alloy has been studied with the help of non-isothermal scanning experiments in a differential scanning calorimeter. The thermograms at different scanning rates show a two-step crystallization. To determine the activation energy, the methods of Kissinger, Ozawa and Boswell are used starting from the shift of the peaks (T_p) according to the heating rate.

(Received June 27, 2012; accepted September 20, 2012)

Keywords: Nickel–Zirconium alloys, Rapid solidification, X-ray diffraction, Differential scanning calorimetry

1. Introduction

Hydrogen-permeable metal membranes generally have high selectivity, permeability and thermal stability, so that they are expected to be used for various industrial applications, including ultra-pure hydrogen production [1].

Metals used for gaseous-hydrogen separation have to meet at least three requirements: high permeability, activity to dissociate hydrogen molecules and resistance to hydrogen embritlement [2, 3].

The palladium and its alloys are well known as the hydrogen permeable metal membranes for the separation and purification of hydrogen gas [4, 5]. However palladium alloys are too expensive for large-scale industrial applications as hydrogen separation membranes. In order to reduce the materials cost as well as to improve the performance of the hydrogen permeability the development of new hydrogen permeable alloys to be substituted for the currently used palladium alloys are needed [6].

Zirconium is one of the most hydrogen-permeable metals because of its high hydrogen diffusivity and solubility [7]. The intrinsic hydrogen permeability of zirconium is higher than that of palladium which has been commercially used for hydrogen purification membranes. However, zirconium has not been recognized as a possible membrane material for hydrogen purification due to hydrogen embritlement problems, especially at low temperatures.

Amorphous alloys are much tougher than the crystalline ones and are often unchanged in a hydrogen atmosphere [8-12]. Furthermore, it is known that amorphous alloys do not show the α–β phase transition during hydrogen absorption which often causes destruction of the membrane structure. Therefore we have been looking for an amorphous alloy which can be used for gaseous hydrogen separation consisting of cheap metals only. Due to their low cost, high strength and resistance to hydrogen embritlement, amorphous Ni-based alloy membranes have received much attention in recent years. The Ni64Zr36 alloy is a good candidate for the hydrogen separation application, since it doesn't need a dissociation catalyst and contains common metals, shows a very favorable hydrogen output per material cost compared to Pd, but questionable thermal stability above 300°C. Yamaura [13] showed that the partial substitution of Zr by other early transition metals (ETM) changed both the crystallization temperatures and hydrogen permeability, with the change in measured crystallization temperature being roughly dependent on the bond energy of the substitute element.

The amorphous state is a high energy (metastable) state. Consequently, they tend lower their energy by transforming into the crystalline state, a process referred to as crystallization. The crystallization is expected to take place at or above the crystallization temperature, T_x, which is measured by thermal analysis during continuous heating of the material at a constant heating rate.

The study of the crystallization behavior of the amorphous alloy is very interesting from a scientific point of view but also from technological point too. Studies on the crystallization behavior of metallic glasses provide an opportunity to study the kinetics of crystallization and the acting micro mechanisms to. Such results will provide a

clear understanding of the way the metallic glass transforms into the crystalline state and offer a means to impede and control the crystallization behavior.

From a technological point of view, the crystallization temperature of metallic glasses provides a real upper limit to the safe use of the amorphous metallic membranes without losing their interesting combination of properties.

The main barrier towards use of these materials is the thermal stability, since such alloys show a tendency to crystallize after exposure to elevated temperatures. As crystallization results in a decrease in hydrogen permeability [8-11], a loss of strength and an increase in susceptibility to hydrogen embritlement, the upper temperature limit at which an amorphous alloys membrane can operate is dictated by the time–temperature–transformation (TTT) relationship of that alloy.

Differential scanning calorimetry (DSC) has become a convenient and widely used tool for studying the kinetics of phase transformations. The kinetic data on the phase transformation can be obtained from this technique in either the isothermal or linear heating (scanning) mode.

Thermal stability is often referred to in terms of the reduced glass transition temperature ($T_{rg} = T_g/T_m$, where T_g is the glass transition temperature, and T_m is the melting temperature), or by the width of the supercooled region ($T_X - T_g$, where T_X is the crystallization temperature). For the purposes of this application, the upper operational limit is defined by the onset of glass transition, or the crystallization temperature for materials with no clearly defined T_g. Amorphous alloys that do not exhibit a glass transition are not glasses. However, comparison of the glass transition temperature of a metallic glass with the crystallization temperature of an amorphous alloy measured at high heating rates enables a comparison of thermal stability of the two materials [14]. T_g and T_x are therefore the primary measure of glass stability for this application, and offer the primary means by which candidate alloys can be screened.

Another important parameter which defines the thermal stability is the activation energy for crystallization. As the activation energy represents the energy needed for rearranging the atoms during crystallization one can expect that the higher the activation energy is the higher the stability of the amorphous state is. The most commune methods for determining the activation energy are based on the shift of the picks when using different heating rates [15-17].

The present work focuses on the obtaining and characterization of amorphous Ni62Zr37Al1 tapes (in at. %).

2. Experimental methods

The master alloys were prepared by arc melting using high purity metals in a Ti-gettered argon atmosphere. The alloys were melted several times in order to improve homogeneity. The alloy ingot was induction-melted under a high-purity argon atmosphere in a quartz crucible and injected through a nozzle onto a rotating Cu wheel to produce amorphous tapes. The rotation speed used during the present experiments was 32 m/s. The obtained tapes were 4 mm wide and approximately 40 μm thick and presented an amorphous structure. The crystallization of the alloys was evaluated using DSC measurements (heating rate 10, 20, 30 and 40 K/min). To determine the activation energy, the methods of Kissinger, Ozawa and Boswell [15-17] are used starting from the shift of the exothermic peak (T_x) according to the heating rate. Stress–strain curves were measured at room temperature using a tensile testing machine on a 150 mm-long tape using a loading speed of 0.2 mm/min.

3. Results and discussion

Fig. 1 shows the X-ray diffraction pattern of as-melt-spun ribbon. There are no sharp peaks present to indicate the presence of a crystalline phase; the amorphous nature of the obtained material is demonstrated by the presence of a wide peak centered on the 2θ angle of 41.5°. The full with at half maximum is 6.1°.

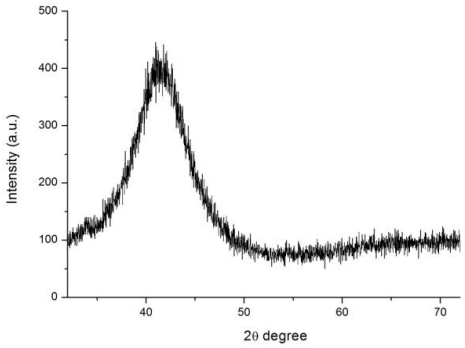

Fig. 1. X-ray diffraction pattern of a Ni64Zr36 amorphous ribbon.

The crystallization behavior of the obtained ribbons was studied using linear heating DSC experiments. Such a curve obtained using the heating rate of 20 K/min is presented in Fig. 2. Four thermal effects (three exothermic (418.7°C, 559°C and 576.9°C) and one endothermic (1082°C)) were observed, but no clear glass transition was present.

Table 1. Thermal stability of some Ni64Zr36 type alloys [18].

Alloy	T_x (°C)	T_m °C)	T_r (°C)
Ni64Zr36	569	1069	0.53
Ni64Zr26Hf10	569	1099	0.52
Ni64Zr26Nb10	602	1100	0.55
Ni64Zr26Ta10	572	1128	0.51
Ni64Zr26Ti10	568	1023	0.56
Ni62Fe1Zr37 *	542	1061	0.51

** present study*

Since no glass transition is observed we used the reduced crystallization temperature ($T_r=T_x/T_m$) [19] in

order to compare the alloys glass forming ability (GFA) and his thermal stability with other Ni-Zr type alloys. As it is well known [20], the Ni-Zr system has the best glass forming ability around 35 at. % Zr. The main factor that influences the thermal stability is the bond energy. The Ni64Zr36-x type alloys (Table 1) confirms it very well.

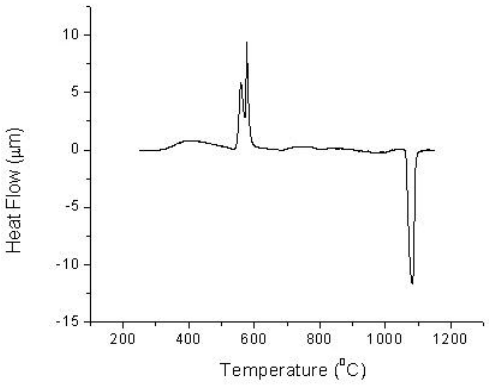

Fig. 2. DSC curve of the as-quenched Ni-Zr alloy (heating rate 20K/min).

In the case of our alloy this alone cannot explain the reduction of the glass forming ability due to the small increase in the bond valence. The second effect which acts as a GFA reducers are the geometric effects. Since the Fe atom has an atomic radius (0.1241) close to that of the Ni atom (0.1246).

In order to determine the nature of the effects observed here, the DSC measurements were stopped at different temperatures and subjected to X-ray analysis.

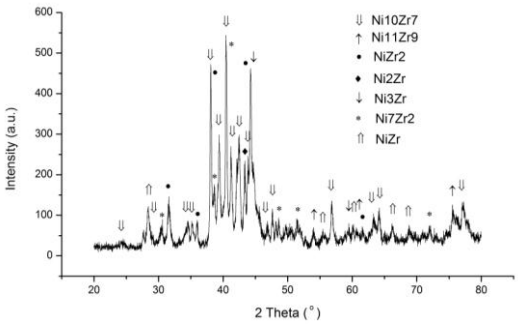

Fig. 3. X-ray diffraction pattern of a Ni64Zr36 alloy heat treated at 800 °C.

After a DSC analysis and heat treatment at 800 °C the samples were studied by X-ray diffraction. An obtained X-ray pattern is presented in Fig. 3. The presence of a number of phases were identified. Around the Ni64Zr36 eutectic composition the driving force for crystallization is close for different phases [20]. As a result, in the X-ray diffraction pattern, the presence of multiple components is observed. The maximum driving force is for $Ni_{10}Zr_7$ and $Ni_{11}Zr_9$ while the compounds $NiZr_2$ and Ni_5Zr have the lowest.

The thermal stability of the ribbons was assessed by the activation energy for crystallization; the methods of Kissinger, Ozawa and Boswell are used to determine the activation energy from the change of the temperature corresponding to the maximum of the exothermic peak when using different heating rates. In our experiments, the heating rates were chosen as 20, 30 and 40 K/min in order to separate the two crystallization effects. The crystallization temperature was considered the maximum of the observed peak.

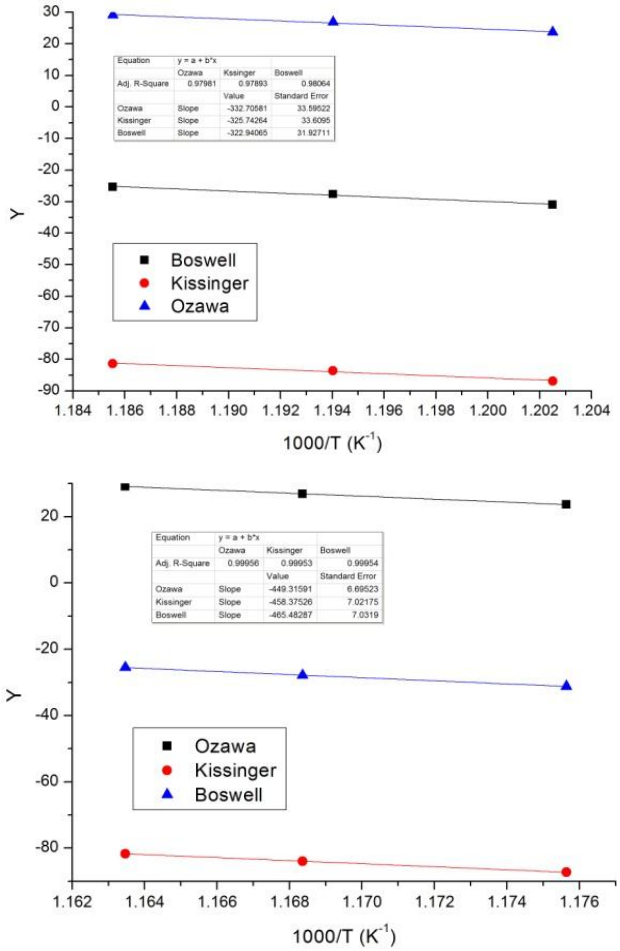

Fig. 4. Y=f (1000/Tm) curves using the three different methods for both crystallization effects.

$$Y=R\cdot\ln(\alpha/T_m^2)= - E_a/T_m + C \quad \text{Kissinger ecuation} \quad (1)$$

$$Y= R\cdot(\ln\alpha)/1.0518 = - E_a/T_m + C_1 \quad \text{Ozawa ecuation} \quad (2)$$

$$Y= R\cdot\ln(\alpha/T_m)= - E_a/T_m + C_2 \quad \text{Boswell ecuation} \quad (3)$$

T_m is the maximum of the exothermic peak, α, the heating rate, C, C_1 and C_2 are constants, E_a is the activation energy and R the perfect gas constant.

Table 2. Crystallization temperatures at heating rate of 20K/min and activation energies for crystallization (E_a).

Peak	Temperature °C	E_a (Ozawa) kJ/mol.	E_a (Kissinger) kJ/mol	E_a (Boswell) kJ/mol.
X1	558.6	332.7	325.7	322.9
X2	577.6	449.3	458.4	465.5

By plotting Y versus 1/(T), an approximately straight line will be obtained. If T_m for different heating rates is chosen, the activation energy E_a can be calculated from the slope of the line. Using these data, the activation energies for crystallization were calculated from the DSC data and presented in Table 2.

The mechanical behavior of the tapes was studied using stress-strain curves; such a curve is presented in Fig. 5. The obtained tapes present a small deformation (0.8%) and a tensile strength around 200 MPa. The Young's modulus, defined as the ratio of the uniaxial stress over the uniaxial strain in the range of stress in which Hooke's law holds, is 27.5 GPa.

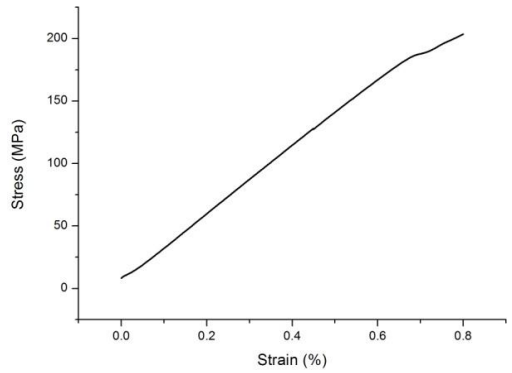

Fig. 5. Stress-strain curve of an amorphous ribbon.

Significant deviations can occur in the values of the tensile strength due to the fact that the specimens used for testing were not prepared in a special way; the as obtained tapes were used. The defects and irregularities present on the specimens margins act as tension concentrators causing premature rupture of the samples.

4. Conclusions

The amorphous nature of the obtained material is demonstrated by the presence of a wide peak centered on the 2θ angle of 41.5°.

The crystallization behavior of the obtained ribbons was studied using linear heating DSC experiments. Two exothermic effects were observed. These two peaks correspond to a complex crystallization of a number of phases of the Ni-Zr system.

The mechanical behavior of the tapes was studied using stress-strain curves. The obtained tapes present a small deformation (0.8%) and a tensile strength around 200 MPa. The Young's modulus, defined as the ratio of the uniaxial stress over the uniaxial strain in the range of stress in which Hooke's law holds, is 27.5 GPa.

Acknowledgements

This paper was supported by the projects "Doctoral studies in engineering sciences for developing the knowledge based society – SIDOC" contract no. POSDRU/88/1.5/S/60078, project co-funded from European Social Fund through Sectorial Operational Program Human Resources 2007-2013 and "Development and support of multidisciplinary postdoctoral programmes in major technical areas of national strategy of Research - Development - Innovation"4D-POSTDOC, contract no. POSDRU/89/1.5/S/52603, project co-funded by the European Social Fund through Sectoral Operational Programme Human Resources Development 2007-2013.

References

[1] S. Hara, N. Hatakeyama, N. Itoh, H-M. Kimura, A. Inoue, Journal of Membrane Science **211**, 149 (2003).
[2] C. Nishimura, M. Amano, M. Komaki, Mater. Trans., JIM, **32**, 501 (1991).
[3] S. Hara, K. Sakaki, N. Itoh, H-M. Kimura, K. Asami, A. Inoue, Journal of Membrane Science **164**, 289 (2000).
[4] W. H. Chen, I. H. Chiu, International Journal of Hydrogen Energy, **34**, 2440 (2009).
[5] S. N. Paglieri, J. D. Way, Sep. Purif. Methods. **31**, 1 (2002).
[6] T. Ozaki, Y. Zhang, M. Komaki, C. Nishimura, International Journal of Hydrogen Energy, **28**, 1229 (2003).
[7] R. E. Buxbaum, T. L. Marker, Journal of Membrane Science, **85**, 29 (1993).
[8] C. Nishimura, M. Komaki, S. Hwang, M. Amano, J. Alloy. Compd., **330 –332**, 902 (2002).
[9] S. Yamaura, K. Isogai, H. Kimura, A. Inoue, J. Mat. Res., **17**, 60 (2002).
[10] S. Yamaura, H. Kimura, A. Inoue, Mater. T. JIM., **44**, 1885 (2003).
[11] S. Yamaura, Y. Shimpo, H. Okouchi, M. Nishida, O. Kajita, A. Inoue, Mater. T. JIM., **45**, 330 (2004).
[12] S. Yamaura, M. Sakurai, M. Hasegawa, K. Wakoh, Y. Shimpo, M. Nishida, H.Kimura, E. Matsubara, A. Inoue, Acta Mater. **53**, 3703 (2005).
[13] S. Yamaura, S. Nakata, H. Kimura, Y. Shimpo, M. Nishida, A. Inoue, Mater. T., **46**, 1768 (2005).
[14] M. D. Dolan, N. C. Dave, A. Y. Ilyushechkin, L. D. Morpeth, K. G. McLennan, J. Membr Sci **285**, 30 (2006).
[15] H. E. Kissinger, Anal. Chem., **29**, 1702 (1957).
[16] T. Ozawa, J. Therm. Anal., **2**, 301 (1970).
[17] P. G. Boswell, J. Thermal Anal., **118**, 353 (1980).
[18] M. D. Dolan, S. Hara, N. C., K. Haraya, M. Ishitsuka, A. Y. Ilyushechkin, K. Kita, K. G. McLennan, L. D. Morpeth, M. Mukaida, Sep. Purif. Technol., **65**, 298 (2009).
[19] A. Tekeuchi, A. Inoue, Mater. T., **43**, 2275 (2002).
[20] T. Abe, M. Shimono, M. Ode, H. Onodera, J. Alloys Comp. **434–435**, 152 (2007).

* Corresponding author: Lorand.Bukkosi@stm.utcluj.ro